PACS numbers: 42.62.Cf; 42.60.Jf; 42.25.Ja
DOI: 10.1070/QE2005v035n02ABEH002728

Numerical analysis of the effect of the TEM_{00} radiation mode polarisation on the cut shape in laser cutting of thick metal sheets

A.V. Zaitsev, O.B. Kovalev, A.M. Orishich, V.M. Fomin

***Abstract*. The effect of polarisation of a Gaussian beam on the radiation absorption during laser cutting of metals is investigated. A generalised formula is proposed for calculating the absorption coefficient, which describes the polarisation of three types (linear, elliptical, and circular), taking into account the fact that the beam may interact with a metal surface of an arbitrary shape. A comparison with the existing analogues (in the cases of linear and circular radiation polarisation) confirmed the advantage of employing the formula for the spatial description of the shape of the surface produced, which is highly important for processing (cutting, welding, drilling) of thick materials. The effect of laser radiation characteristics on the surface shape and cut depth in cutting stainless steel sheets is investigated numerically. It is shown for the first time that the cutting of materials by the TEM_{00} beam is most efficient when the beam has elliptical polarisation directed along the direction of beam displacement and characterised by a specific axial ratio.**

Keywords: *polarisation of laser radiation, absorption coefficient, laser cutting, thick materials, mathematical simulation.*

1. Introduction

With the recent advent of new industrial lasers with an output power up to 10 kW [1] and the development of automated laser technological complexes on their basis [2], the technologies of laser cutting of thick materials (up to 20 – 30 mm in thickness) have been developed [3, 4]. This stimulated the development of more sophisticated mathematical methods for describing the laser radiation – metal interaction to find the optimal conditions for high-quality material processing. In the published works on this subject [5 – 9], the effects of radiation characteristics on the absorption coefficient and the shape of metal surface produced in the process of cutting have not been adequately investigated. In particular, the well-known expressions commonly used in the literature for calculating the absorption coefficient for linearly and circularly polarised Gaussian beams are inapplicable for describing the interaction of radiation with material surface of an arbitrary shape. Such a description becomes utterly urgent in the simulation of laser machining of thick metal sheets.

A.V. Zaitsev, O.B. Kovalev, A.M. Orishich, V.M. Fomin Institute of Theoretical and Applied Mechanics, Siberian Branch, Russian Academy of Sciences, ul. Institutskaya 4/1, 630090 Novosibirsk, Russia

Received 9 June 2004; revision received 26 October 2004
Kvantovaya Elektronika **35** (2) 200 – 204 (2005)
Translated by E.N. Ragozin

2. Formulation of the problem

Let us assume that the radiation energy during cutting is spent only on metal heating and melting (the solid material evaporation and the radiation – vapour interaction are neglected), the melt is removed by neutral-gas blowing, the melt film thickness at the cut front is negligible, the absorption coefficient is independent of the temperature, and only single absorption of radiation is taken into account. The traditional formulation of the problem on the transformation of a free material surface exposed to laser radiation reduces to the kinematic consistency equation for the points of the surface [6 – 8]:

$$\frac{\partial z_\mathrm{m}}{\partial t} - V_\mathrm{c}\frac{\partial z_\mathrm{m}}{\partial x} = -V_\mathrm{n}\left[1 + \left(\frac{\partial z_\mathrm{m}}{\partial x}\right)^2 + \left(\frac{\partial z_\mathrm{m}}{\partial y}\right)^2\right]^{1/2}, \quad (1)$$

$$z_\mathrm{m}(x, y, 0) = 0, \quad (2)$$

$$\frac{\partial z_\mathrm{m}}{\partial x}(-\infty, y, t) = \frac{\partial z_\mathrm{m}}{\partial x}(\infty, y, t) = 0,$$
$$\frac{\partial z_\mathrm{m}}{\partial y}(x, -\infty, t) = \frac{\partial z_\mathrm{m}}{\partial y}(x, \infty, t) = 0, \quad (3)$$

where t is the time; x, y, and z are the spatial coordinates; $z = z_\mathrm{m}(x, y, t)$ is the equation of the surface; V_c is the beam displacement speed (or the cutting speed) directed along the x axis.

The normal component V_n of the surface motion velocity can be calculated by using a local conservation law [6, 7]. We will use an analogue of this law, which we obtained [10] taking into account the temperature dependences of material density and heat capacity:

$$V_\mathrm{n} = Q\left[\rho_\mathrm{m}H_\mathrm{m} + c_\mathrm{s}^0\rho_\mathrm{s}^0(T_\mathrm{m} - T_0)\int_0^1 v(\tau)\mathrm{d}\tau\right]^{-1}, \quad (4)$$

$$Q = AI(x, y, z)\cos\gamma,$$

where A is the absorption coefficient; $I(x, y, z)$ is the radiation power density; γ is the angle of ray incidence; ρ_m is the material density at the melting temperature T_m; H_m is the specific heat of melting; ρ_s^0 and c_s^0 are the material

density and specific heat capacity at the initial temperature T_0. The function $\nu(\tau)$, where $\tau = (T - T_0)/(T_m - T_0)$, takes into account the temperature dependence of the product of the metal density by the heat capacity [10].

We consider the cw radiation from a CO_2 laser at a wavelength of 10.6 μm. The radiation intensity is described by the Gaussian distribution, which corresponds to the TEM_{00} mode [11]:

$$I(x,y,z) = \frac{2W}{\pi\omega_z^2}\exp\left(-\frac{2r^2}{\omega_z^2}\right), \qquad (5)$$

$$\omega_z = \left\{\omega_0^2 + \left[\frac{(z-z_f)\lambda_0}{\pi\omega_0}\right]^2\right\}^{1/2}, \quad r = \left(x^2+y^2\right)^{1/2},$$

where W is the radiation power; z_f is the distance between the $z = 0$ plane and the focal plane; and ω_0 is the beam radius in the focal plane.

By using the well-known Fresnel equations [12], the expressions for the reflection coefficients can be written in the form

$$R_s = \left|\frac{\cos\gamma - \left(N_\omega^2 - \sin^2\gamma\right)^{1/2}}{\cos\gamma + \left(N_\omega^2 - \sin^2\gamma\right)^{1/2}}\right|^2,$$
$$R_p = \left|\frac{N_\omega^2\cos\gamma - \left(N_\omega^2 - \sin^2\gamma\right)^{1/2}}{N_\omega^2\cos\gamma + \left(N_\omega^2 - \sin^2\gamma\right)^{1/2}}\right|^2, \qquad (6)$$

where R_s and R_p are the reflection coefficients for the waves polarised perpendicular (the s-wave) and parallel (the p-wave) to the plane of incidence; $N_\omega = n_\omega + i\varkappa_\omega$ is the complex refractive index; n_ω is the refractive index; and $\varkappa_\omega$ is the absorption coefficient.

Consider the case of a linearly polarised Gaussian beam. Figure 1 shows a surface element oriented at an angle to the x axis of the Cartesian coordinate system xyz. The wave vectors of the incident ($\boldsymbol{k}$) and reflected ($\boldsymbol{k}_r$) radiation as well as the unit vector of the normal $\boldsymbol{N}$ to the surface form the plane of incidence. The vector $\boldsymbol{k}$ is parallel to the z axis. The electric field vector $\boldsymbol{E}$ is decomposed into two projections. To the projection $\boldsymbol{E}_p$, which lies in the plane of incidence, the reflection coefficient R_p corresponds and to the projection $\boldsymbol{E}_s$, which is perpendicular to the plane of incidence, the reflection coefficient R_s. Let β be the angle between the $\boldsymbol{E}$ vector and the normal to the plane of incidence $\boldsymbol{N}_{kn} = \boldsymbol{N}\times\boldsymbol{k}/|\boldsymbol{k}|$, then $\boldsymbol{E}_p = \boldsymbol{E}\sin\beta$ and $\boldsymbol{E}_s = \boldsymbol{E}\cos\beta$. Because the vector $\boldsymbol{k}$ is directed along the unit vector $\boldsymbol{e}_z$, while the $\boldsymbol{E}$ vector is perpendicular (or parallel) to the beam motion, $\cos^2\beta = N_x^2$ (or $\cos^2\beta = N_y^2$), where N_x and N_y are the components of the normal to the surface. According to [13], the expression for the absorption coefficient is written in the form

$$A(\gamma,\beta) = 1 - R(\gamma,\beta) = 1 - \frac{I_r}{I_0} = 1 - \frac{E_r^2}{E^2}$$
$$= 1 - \frac{R_p(\gamma)E_p^2 + R_s(\gamma)E_s^2}{E^2} = 1 - R_s(\gamma)\cos^2\beta - R_p(\gamma)\sin^2\beta, \qquad (7)$$

where I_r and I_0 are the reflected and incident radiation intensities, which are proportional to the squared intensities of the electric fields E_r and E, respectively. Figure 2 shows the dependences of the coefficient A on the angle of incidence γ for different β. For $\beta = \pi/2$ we will have a linear p-wave and for $\beta = 0$ a linear s-wave.

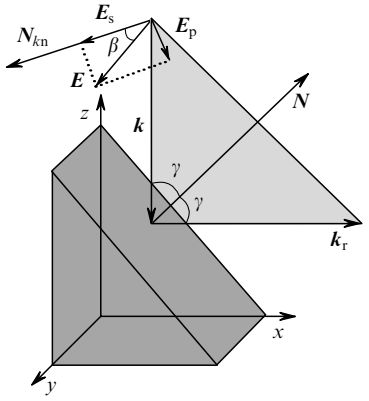

Figure 1. Scheme of the interaction of a beam with a surface element.

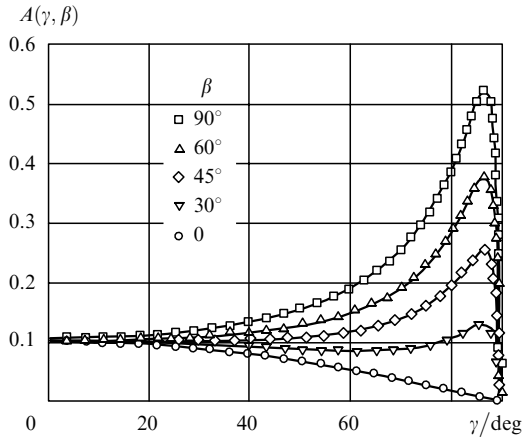

Figure 2. Dependences of the absorption coefficient A on the angles γ and β for linearly polarised radiation.

Consider now the case of elliptical beam polarisation, when the end of the vector $\boldsymbol{E}$ in the xy plane circumscribes an ellipse with the semiaxes a and b oriented parallel to the x and y axes. In this case, the relation $a^2 + b^2 = 1$ is satisfied. We write the expression for the absorption coefficient in the form $A = a^2A_x + b^2A_y$, where A_x and A_y are the absorption coefficients for the radiation polarised parallel to the x and y axes. According to expression (7), we obtain

$$A_x(\gamma,\beta_x) = 1 - R_s(\gamma)\cos^2\beta_x - R_p(\gamma)\sin^2\beta_x,$$
$$A_y(\gamma,\beta_y) = 1 - R_s(\gamma)\cos^2\beta_y - R_p(\gamma)\sin^2\beta_y, \qquad (8)$$

where β_x and β_y are the angles between the normal to the plane of incidence $\boldsymbol{N}_{kn}$ and the x and y axes, respectively. The angles β_x and β_y satisfy the equalities:

$$\cos^2\beta_x = \left[\left(\frac{\boldsymbol{k}}{|\boldsymbol{k}|}\times\boldsymbol{N}\right)\boldsymbol{e}_x\right]^2 = (\boldsymbol{N}\boldsymbol{e}_y)^2 = N_y^2,$$
$$\cos^2\beta_y = \left[\left(\frac{\boldsymbol{k}}{|\boldsymbol{k}|}\times\boldsymbol{N}\right)\boldsymbol{e}_y\right]^2 = (\boldsymbol{N}\boldsymbol{e}_x)^2 = N_x^2. \qquad (9)$$

By substituting (9) into (8), we obtain the expression for the absorption coefficient in the case of elliptical polarisation:

$$A(\gamma, \boldsymbol{N}) = a^2 A_x + b^2 A_y = 1 - R_s\left(a^2 N_y^2 + b^2 N_x^2\right)$$

$$- R_p\left[a^2\left(1 - N_y^2\right) + b^2\left(1 - N_x^2\right)\right]. \quad (10)$$

The absorption coefficient A depends strongly on the angle of incidence, the spatial orientation of the surface normal vector, and the radiation polarisation, which is characterised by ellipse axial ratio b/a.

Let us analyse expression (10). For $a = b = 1/\sqrt{2}$, we have circularly polarised radiation. In view of the equality $N_x^2 + N_y^2 + N_z^2 = 1$, we obtain from (10) the expression for the absorption coefficient:

$$A_c = 1 - \frac{R_s\left(1 - N_z^2\right) + R_p\left(1 + N_z^2\right)}{2}. \quad (11)$$

Let us assume that the material surface being cut is such that the cut front and the side walls depart only slightly from the vertical. For thin sheets (up to 1–3 mm in thickness), this fact is confirmed experimentally. In this case, the component N_z of the normal vector $\boldsymbol{N}$ is close to zero. Then, from expression (11) it is easy to obtain, by setting $N_z = 0$, that $A_c = 1 - 0.5(R_s + R_p)$. This is the well-known expression commonly employed in the literature for approximate estimates of the absorption coefficient for circular polarisation.

For $a = 1$ and $b = 0$ we have a linear p-wave (i.e. a wave polarised parallel to the direction of cutting), and we obtain from (10)

$$A_p = 1 - R_p + N_y^2(R_p - R_s). \quad (12)$$

Note that it follows from (12) for $N_y = 0$ that $A_p = 1 - R_p$. This expression is also widely used in the literature to calculate the absorption coefficient for a parallel radiation polarisation; according to (10), this expression adequately describes absorption at only one frontal line of the cut where the normal vector $\boldsymbol{N}$ may have nonzero components N_x and N_y. This is possible if the cut width is very small.

Finally, if $a = 0$ and $b = 1$ we have a linear s-wave (i.e. a wave polarised perpendicular to the direction of cutting) and find from (10)

$$A_s = 1 - R_p + N_x^2(R_p - R_s). \quad (13)$$

By setting $N_x = 1$ in (13), we obtain the relation $A_s = 1 - R_s$, which is used in the literature to calculate the absorption coefficient for perpendicular polarisation. This relation can adequately describe absorption only at the points of the cut front, where $N_y = 0$ and $N_z = 0$.

Therefore, relations (10)–(13) allow the calculation of the absorption coefficient for elliptical (10), circular (11), and linear (12), (13) radiation polarisations in the general case of an arbitrarily shaped material surface.

3. Results of calculations and discussion

We used in our calculations the physical parameters of stainless steel given below.

Melting temperature T_m/K	1700
Specific heat capacity c_s^0/J kg^{-1} deg^{-1}	477
Density/kg m^{-3}:	
ρ_s^0 for the initial temperature $T_0 = 300$ K	7870
ρ_m^0 for the melting temperature T_m	6610
Specific heat of melting H_m/kJ kg^{-1}	276
Refractive index n_ω	17.87
Absorption coefficient $\varkappa_\omega$	4.2

Equation (1) with initial (2) and boundary (3) conditions and closure relations (4)–(8) and (12) was numerically solved by the pseudotransient method using an explicit second-order difference scheme [14]. Within the framework of the formulated problem (1)–(3), the cut surface is measured from the upper plane of the metal sheet $z = 0$ to the maximum material damage depth $z < 0$. The main part of the radiation interacting with the metal is incident on the cut surface at large angles. The principal feature in this case is a strong dependence of the absorption coefficient on the angle of incidence (Fig. 2).

The results of a series of numerical experiments on the determination of the maximum cut depth L as a function of the axial ratio b/a of the ellipse are presented in dimensionless variables $(L/\omega_0, b/a)$ in Fig. 3 for different values of the dimensionless parameter $\sigma = 2W\{\pi\omega_0^2 V_c[\rho_m H_m + \rho_s^0 c_s^0(T_m - T_0)]\}^{-1}$. The maximum cut depth for circularly polarised radiation ($b/a = 1$) turned out to be much greater than for linearly polarised radiation ($b/a = 0$). The calculated dependences exhibit a distinct maximum, which corresponds to elliptically polarised beam with the axial ratio $b/a = 0.75-0.8$. The curves in Fig. 3 exhibit oscillations caused by the computational method, which can be removed by using a higher-order difference scheme. The typical shape of a laser cut obtained by using an elliptically polarised beam is shown in Fig. 4. The horizontal level lines correspond to the contour of the produced surface. The maximum cut depth is about 10 mm.

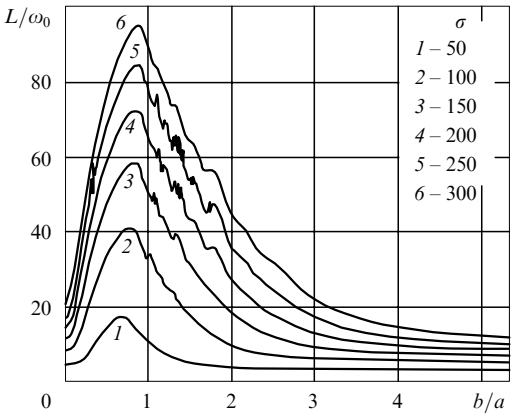

Figure 3. Dependences of the maximum normalised cut depth L/ω_0 on the ellipse axial ratio b/a for different parameters σ.

The isolines of the absorption coefficient $A[x, y, z_m(x, y)]$ for linearly (a, b) and circularly (c) polarised beams in the xy plane are plotted in dimensionless coordinates in Fig. 5. The dimensionless parameter is $\sigma = 300$, which corresponds to a power $W = 2.2$ kW and a cutting speed $V_c = 45$ mm s^{-1}. In the cutting by s-polarised radiation ($b = 1$, $a = 0$), when the electric field vector $\boldsymbol{E}$ is perpendicular to the beam motion,

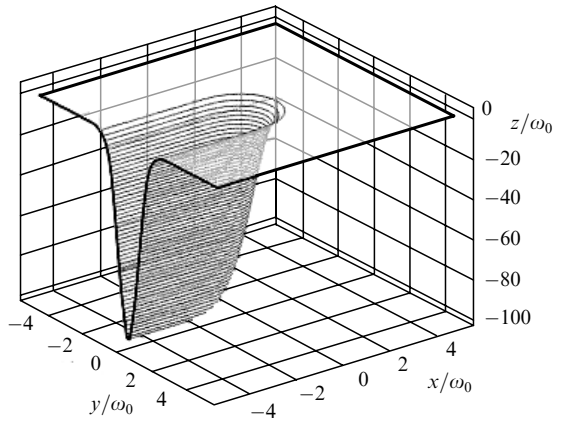

Figure 4. Typical shape of the cut surface $z = z_m(x, y)$ for $\sigma = 300$, $b/a = 0.75$, and $\omega_0 = 100$ μm.

the absorption maximum is located on the side walls (Fig. 5a). The absorption coefficient at the cut front is minimal, and therefore the maximum cut depth is also small. The produced cut is smooth and broad, its depth being about 1 mm, because the maximum absorption coefficient is distributed over the side surface. When cutting is performed with p-polarised radiation ($b = 0$, $a = 1$), the vector $\boldsymbol{E}$ is parallel to the beam motion, the absorption maximum is located on the cut front (Fig. 5b), where the radiation is incident at an angle of $85^\circ - 87^\circ$. The cut turns out to be narrow, its depth being ~ 2 mm, because the greater part of the radiation is reflected from its front and does not penetrate deep into the cut.

For a circular polarisation ($b = a = 1/\sqrt{2}$), the absorption maximum is quite uniformly distributed over the entire cut surface (Fig. 5c) to yield the maximum cut depth of 9 mm. In this case, the side surface evolves to a vertical wall. A very steep slope of the cut walls provides a very strong radiation absorption, which abruptly decreases to zero when the angle of incidence approaches 90°. In all cases, the irradiated surface tends to assume the form providing the weakest radiation absorption.

It is commonly assumed [15, 16] that a linearly polarised p-wave absorbed at the front is most efficient for cutting. In practice, however, circularly polarised radiation is commonly used. This is explained by technical difficulties of controlling the plane of electric vector polarisation in the cutting of intricately shaped pieces [15–17]. Calculations performed in [7, 8] showed that the cutting efficiency of a circularly polarised wave is as good as that of a linearly polarised p-wave. An analysis of the results of calculations presented in Figs 3 and 5 [with the use of more exact expressions (10)–(13) for calculating the absorption coefficient] suggests that the cutting efficiency for circularly polarised radiation is much higher than that for a p-wave. In this case, cutting by elliptically polarised radiation has the highest efficiency.

Therefore, when the TEM_{00} mode is used, the cutting of metal sheets is most efficient for elliptical polarisation oriented along the direction of beam motion and characterised by a certain axial ratio $b/a = 0.75 - 0.8$.

The possibility of existence of a radially polarised beam (r polarisation), which is provided by the superposition of two perpendicular TEM_{01} modes, is discussed in Refs [7–9]. According to [7–9], the advantage of cutting by an r-polarised beam compared to cutting by circularly polarised radiation is that the depth or the cutting speed are greater by a more than a factor of 1.5–2 in the former case. In our opinion, this estimate is not correct, because it was obtained from the physical analysis of the effect of different radiation modes or their combinations on the cut shape and because the calculations of Refs [7–9] were presented only for thin plates (up to 4.5 mm in thickness) and the efficiency was estimated only from the cut depth.

The issues of the feasibility of generating differently polarised high-quality TEM_{01} modes and of the efficiency of radially polarised radiation have not been adequately studied so far. In the TEM_{01}-mode generation, a loss in the output power inevitably occurs (compared to the TEM_{00} mode) and the beam thickness increases, which results in an increase in the cut width.

4. Conclusions

We have investigated the problem of describing the shape of the surface produced in the laser cutting of metals by high-power single-mode laser radiation (the TEM_{00} mode). We derived expression (10) for the calculation of the

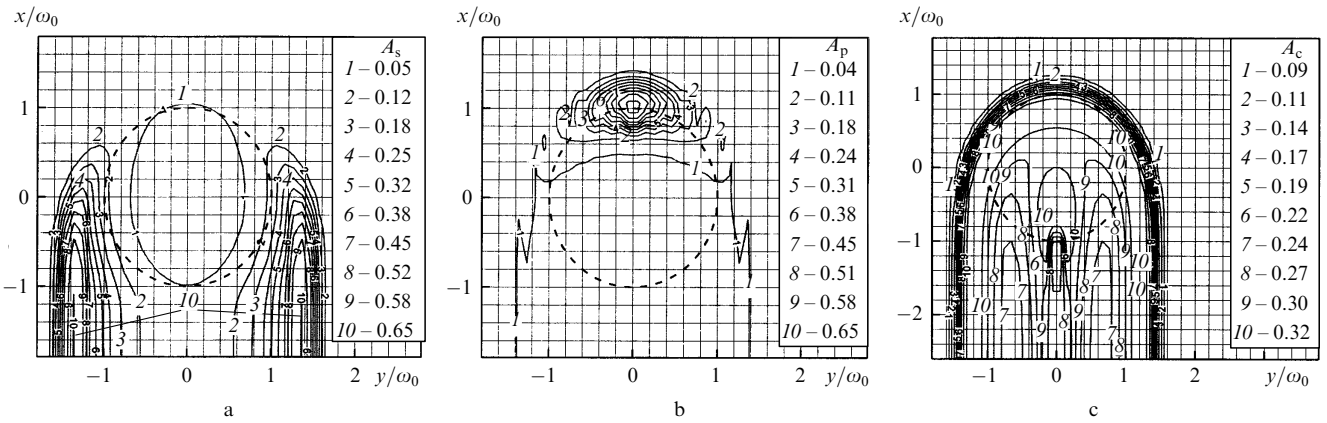

Figure 5. Isolines of the absorption coefficient $A[x, y, z_m(x, y)]$ on a free metal surface for three types of beam polarisation: $A_s = 1 - R_p + N_x^2(R_p - R_s)$, linear s-wave (a); $A_p = 1 - R_p + N_y^2(R_p - R_s)$, linear p-wave (b); and $A_c = 1 - 0.5[R_s(1 - N_z^2) + R_p(1 + N_z^2)]$, circular polarisation (c). The dashed line indicates the beam section at the waist with the radius $\omega_0 = 100$ μm.

absorption coefficient. This dependence takes into account the spatial orientation of the plane of radiation incidence, which is very important for cutting thick materials with a large ratio of the cut depth to the beam diameter. Expression (10) enables calculating the absorption coefficient in the case of elliptical beam polarisation oriented either perpendicular ($a < b$) or parallel ($a > b$) to the beam motion, for an arbitrary b/a ratio. The effect of laser radiation characteristics on the cut depth and surface shape was investigated numerically. We have shown that the radiation with elliptical polarisation oriented along the direction of beam motion and characterised by a certain axial ratio $b/a \approx 0.75$ should possess the highest efficiency.

Acknowledgements. This work was supported by the Russian Foundation for Basic Research (Grant No. 04-01-00798).

References

1. Afonin Yu.V., Golyshev A.P., Ivanchenko A.I., Malov A.N., Orishich A.M., Pechurin V.A., Filev V.F., Shulyat'ev V.B. *Kvantovaya Elektron.*, **34**, 307 (2004) [*Quantum Electron.*, **34**, 307 (2004)].
2. Afonin Yu.V., Golyshev A.P., Ivanchenko A.I., Konstantinov S.A., Maslov N.A., Orishich A.M., Filev V.F., Shikhalev E.G., Shulyat'ev V.B. *Proc. SPIE Int. Soc. Opt. Eng.*, **4900**, 929 (2002).
3. Malov A.N., Malov N.A., Orishich A.M., Shulyat'ev V.B., et al. *Proceedings of the IV International Scientific and Technical Conference 'Laser Technologies and the Means of Their Realisation'* (St. Petersburg: Izd. St. Peterburg State Polytechn. Univ., 2004) pp 39 – 46.
4. Afonin Yu.V., Ermolaev G.V., Malov A.N., Malov N.A., Orishich A.M., Shulat'ev V.B., Pechurin V.A., Filev V.F. *Proc. XII Int. Conf. «Methods of Aerophysical Research»* (Novosibirsk, 2004) pt 3, pp 3 – 9.
5. Vedenov A.A., Ivanov O.P., Chernyakov A.L. *Kvantovaya Elektron.*, **11**, 2397 (1984) [*Sov. J. Quantum Electron.*, **14**, 1587 (1984)].
6. Cherepanov G.P., Cherepanov A.G. *Fiz. Khim. Obrab. Mater.*, (2), 133 (1990).
7. Nesterov A.V., Niz'ev V.G. *Izv. Ross. Akad. Nauk, Ser. Fiz.*, **63**, 2039 (1999).
8. Niziev V.G., Nesterov A.V. *J. Phys. D: Appl. Phys.*, **32**, 1455 (1999).
9. Nesterov A.V., Niziev V.G. *J. Phys. D: Appl. Phys.*, **33**, 1817 (2000).
10. Kovalev O.B., Orishich A.M., Fomin V.M., Shulyat'ev V.B. *Zh. Prikl. Mekh. Tekhn. Fiz.*, **42**, 106 (2001).
11. Oraevskii A.N. *Tr. Fiz. Inst. Akad. Nauk SSSR*, **187**, 3 (1988).
12. Stuart E., Rutt H.N. *J. Phys. D: Appl. Phys.*, **22**, 901 (1989).
13. Born M., Wolf E. *Principles of Optics* (Oxford: Pergamon Press, 1969; Moscow: Mir, 1973).
14. Samarskii A.A. *Teoriya raznostnykh skhem* (Theory of Difference Schemes) (Moscow: Nauka, 1977).
15. Vedenov A.A., Gladush G.G. *Fizicheskie protsessy pri lazernoi obrabotke materialov* (Physical Processes in the Laser Material Machining) (Moscow: Energoatomizdat, 1985).
16. Pawell J. *CO_2-Laser Cutting* (London: Springer-Verlag, 1998).
17. Grigor'yants A.G. *Osnovy lazernoi obrabotki materialov* (Principles of Laser Material Machining) (Moscow: Mashinostroenie, 1989).